Nafta-Gaz 2023, no. 2, pp. 71–83, DOI: 10.18668/NG.2023.02.01

Control of capillary instability under hydrodynamic impact on the reservoir

Kontrola niestabilności kapilarnej w warunkach hydrodynamicznego oddziaływania na złoże

Geylani M. Panahov[1], Eldar M. Abbasov[1], Babek N. Sultanov[2]

[1] *Institute of Mathematics and Mechanics of Azerbaijan National Academy of Sciences*
[2] *Institute of Geology and Geophysics of Azerbaijan National Academy of Sciences*

ABSTRACT: The paper presents the results of studies on optimisation of water impact on a reservoir by means of sequential periodic increase in hydrodynamic pressure in order to extract capillary trapped oil. The method provides a coordinated account of both displacement conditions and capacitive-filtration characteristics of fluid-saturated reservoirs. The results of experimental, theoretical and field studies of mass transfer processes in the presence of hydrodynamic nonequilibrium in heterogeneous porous media are presented. This paper considers a case where capillary forces are the determining factor for the displacement of immiscible liquids. Laboratory test results have shown that the formation of CO_2 in the reaction of an alkaline solution with naphthenic components can make an additional contribution to the control of surface tension in porous media. A series of experimental studies were carried out on a core sample model to simulate the oil displacement by in-situ generated CO_2 gas-liquid system. The article offers an analytical and technological solution to the problem of ensuring the value of "capillary number" and capillary penetration corresponding to the most complete extraction of trapped oil by regulating the "rate" of filtration (hydrodynamic injection pressure). The paper presents the field cases of implementing the new reservoir stimulation techniques to increase sweep efficiency. For effective residual oil recovery in fluid flow direction, conditions of stepwise (staged) maintenance of specified hydrodynamic water pressure at the boundary of injection contour are considered. Estimated calculations allow to determine time duration and stage-by-stage control of injection pressure as a requirement for reaching the expected increase in oil recovery.

Key words: capillary, hydrodynamics, carbon dioxide, surface tension, sweep efficiency, oil production.

STRESZCZENIE: W artykule przedstawiono wyniki badań nad optymalizacją oddziaływania wody na złoże poprzez sekwencyjne, okresowe zwiększanie ciśnienia hydrodynamicznego w celu wydobycia kapilarnie zatrzymanej ropy. Metoda ta pozwala w sposób skoordynowany uwzględnić zarówno warunki wyporu, jak i charakterystykę kapilarno-filtracyjną złóż nasyconych cieczą. Przedstawiono wyniki badań doświadczalnych, teoretycznych i praktycznych procesów przenoszenia masy w obecności braku równowagi hydrodynamicznej w heterogenicznych ośrodkach porowatych. W artykule rozpatrywany jest przypadek, w którym siły kapilarne są czynnikiem decydującym o wypieraniu niemieszalnych cieczy. Wyniki badań laboratoryjnych wykazały, że powstawanie CO_2 w reakcji roztworu zasadowego ze składnikami naftenowymi może mieć dodatkowy udział w kontroli napięcia powierzchniowego w ośrodkach porowatych. Przeprowadzono serię badań eksperymentalnych na modelu próbki rdzeniowej w celu symulacji wypierania ropy przez generowany in-situ układ gazowo-cieczowy CO_2. W artykule zaproponowano analityczne i technologiczne rozwiązanie problemu zapewnienia wartości „liczby kapilarnej" i przenikania kapilarnego odpowiadających najbardziej pełnemu wydobyciu zatrzymanej ropy, poprzez regulację „szybkości" filtracji (ciśnienia zatłaczania hydrodynamicznego). W artykule przedstawiono przykłady praktycznego zastosowania nowych technik stymulacji złoża w celu zwiększenia efektywności wydobycia. W celu osiągnięcia efektywnego wydobycia ropy resztkowej w kierunku przepływu cieczy rozważono warunki stopniowego (podzielonego na etapy) utrzymywania określonego ciśnienia hydrodynamicznego wody na granicy konturu zatłaczania. Przeprowadzone obliczenia szacunkowe pozwalają na określenie czasu trwania i etapowego kontrolowania ciśnienia zatłaczania jako warunku osiągnięcia oczekiwanego wzrostu odzysku ropy.

Słowa kluczowe: kapilara, hydrodynamika, dwutlenek węgla, napięcie powierzchniowe, efektywność wydobywania, produkcja ropy naftowej.

Corresponding author: Eldar M. Abbasov, e-mail: *eldar.abbasov@imm.az*

Article contributed to the Editor: 09.11.2022. Approved for publication: 08.02.2023.

Introduction

Immiscible fluid displacement in porous media, as well as investigation of the mechanism behind the associated effects, have been the subject of numerous studies of filtration in oil-saturated reservoirs in order to find ways to reduce the proportion of hard-to-recover oil in the total balance of produced hydrocarbons. Methods and technologies for the recovery of residual reserves are the main objective of tertiary methods for enhancing oil recovery. In all of the above processes, the object of study is the complex structure of the pore space, which significantly affects the hydrodynamics and distribution of the fluids saturating it.

As shown in a number of studies, the determining parameters influencing the structure of the displacement front are the viscosity ratio of the displaced and the displacing fluid $M = \mu_1/\mu_2$ and the capillary number – N (dimensionless similarity parameter, characterizing the ratio of viscous and capillary forces) (Larson et al., 1981; Lenormand et al., 1988; Nakoryakov and Kuznetsov, 1997).

Displacement of high-viscosity oil from the reservoir by-water is accompanied by instability and "fingers" of watering and, as a consequence, water breakthroughs, leading to early watering of well production. In general, considering the complexity of the hydrodynamic, thermal and physical-chemical effects occurring in the displacement process confirms that the flow in the formation of almost any displacement agent under certain conditions can become unstable (Wojnicki, 2017). For example, the displacement of high-viscosity oil in a homogeneous reservoir with a polymer solution, which usually has a frontal drive nature, when taking into account the adsorption of the polymer on the reservoir rock walls and several other physical and chemical processes, becomes unstable at a certain stage (Saffman and Taylor, 1958; Brouwer and Jansen, 2002).

Unsteady effects are also possible in relatively macro homogeneous oil-saturated reservoirs. As a result of high viscosity instability (oil/water viscosity ratios), local breakthroughs of injected water take place, which is reflected in water-free and flowing oil recovery rates. With high residual oil saturation values, significant interface surfaces between oil and water phases are formed in the reservoir. This hydrodynamic situation can be used to implement nonstationary methods of impact on the reservoir during its flooding.

Unsteady processes in reservoirs saturated with high-viscosity oil (more than 100 mPas-s) have a number of features. They are caused by:

1) significantly different response times to hydrodynamic perturbations in different permeability and fluid saturation zones;
2) possible gas release and degassing of oil at redistribution of pressure in the formation.

In line with the positive effect of overflow on diverting flows to residual reservoir zones, oilfield development complications can arise if the dynamics of well mode change are unreasonably chosen. Such complications include:

1) possible change of filtration-volumetric properties of the bottomhole formation zone;
2) formation of unstable displacement front in the reservoir, to the strengthening of partitioning of the reservoir by zones of high and low fluid mobility;
3) fast oil degassing in interlayers.

One of the most reliable recovery techniques for heavy, high-viscosity oils is the use of physico-chemical stimulation. These methods significantly increase the oil recovery factor. The efficiency of hydrocarbon production using such technologies consists in a sharp decrease in the viscosity of heavy oils, reducing the surface tension, increasing the temperature in the contact zone, etc. (Sabitov and Sharafutdinov, 1999; Surguchev et al., 2002; Amaral Anderson et al., 2008; Pasquier et al., 2017; Czupski et al., 2020).

For many years, technologies based on the use of chemicals added to injected water have been used in oil production to change the wetting characteristics of the porous medium and the surface tension at the interface of the displaced and displaced fluids. At the late stage of oil field development, aqueous alkali solutions are widely used as displacing agents. Concentrated alkali solutions change wetting characteristics of the porous medium of the oil reservoir and, consequently, create favourable conditions for leaching and emulsifying asphaltene components of highly viscous oils. Stimulation methods on mature oil-saturated reservoirs are based on the effects of alkali reacting with the porous medium of oil reservoir and saturated fluids. The efficient displacing capability of alkaline solutions and their influence on interfacial properties of oil, water and rocks have been known for many years (Nowak, 1953; Rudin and Wasan, 1992; Clark and Kleinberg, 2002; Lyu et al., 2018; Czupski et al., 2020). Considerable interest in the use of alkaline solutions in the waterflooding of depleted oil fields has arisen in recent years in the context of studies of the content of organic and heterorganic compounds in oil – a number of low- and medium molecular weight carboxylic and naphthenic acids; high-molecular-weight resins and asphaltenes, as well as various organic compounds. In addition, Jones et al., (2001) and Wu et al., (2019) found polycyclic aromatic as well as naphthenic-aromatic acids in the composition of high-molecular-weight acids of heavy oils (Yin et al., 2019).

Similar phenomena of reduction of interfacial tension at the "hydrocarbon fluid – organic acids – alkaline solution" boundary and the associated phenomena of self-emulsification

were studied by Phukan et al., (2019). A theoretical justification for the reduction of interfacial tension during the formation of a new substance at the interface was given by Phukan et al., (2019) and Vavra et al., (2020).

Studies have shown that aqueous alkali solutions at the boundary of contact with oil of productive formations lead to a significant reduction in surface tension and have greater activity than solutions of chemical agents currently in use (Islam, 1991; Arekhov et al., 2020). Data obtained by tensometric measurement demonstrate reduction of surface tension at the boundary with oil from 32.0 to 1.0 mN/m at alkali concentration in water, equal to 0.1%.

The results of numerous studies on the methods of alkaline flooding (Taylor et al., 1990; Rudin and Wasan, 1992; Musayev et al., 1999; Liu et al., 2007; Saha et al., 2018) confirm that insufficient attention is paid to the interaction of alkaline solutions based on sodium bicarbonate (Na_2CO_3) with active acidic components in highly resinous heavy oils. The content of naphthenic acids in oils can be quite high (Cheshkova et al., 2019; Rudin and Wasan, 1992). In contact with alkaline fluids, naphthenic acids form water-soluble salts, which are surface-active substances and reduce the surface tension at the oil-water interface. In the course of these studies, it was assumed that along with the well-known effects of reducing interfacial tension, oil emulsification, changes in rock wettability, alkaline flooding has a significant effect on the surface effects in the pore space of the reservoir, accompanied by the effects of interaction of solutions with active acidic components of oil.

Lab experiments

Laboratory experiments were based on the assumption that a carbon dioxide gas (CO_2) is released in the porous medium, a gas-liquid system is formed when an aqueous alkali solution reacts chemically with the active components of heavy oils (naphthenic, carboxylic, organic acids, etc.):

$$RCOOH + NaHCO_3 = RCOONa + H_2O + CO_2\uparrow$$

In the experiments, oil samples from the Binagadi North oil field (Azerbaijan) (GD5 ABCD formation) were used as a model oil with the following characteristics: density 932–940 kg/m^3, viscosity: 99.8–99.9 mPa·s; content of organic acids: 0.5–1 mg KOH/g.

The interfacial tension of solutions (σ) at the interface with the oil was preliminarily determined. Figure 1 shows isotherms of surface tension of caustic and soda ash solutions. From the above dependences of the surface tension value on the type and concentration of alkalis we can conclude that the reaction of the studied reagents with oil leads to a significant decrease in surface tension (from 0.8 to 0.0014 mN/m).

The maximum decrease in surface tension happens at a concentration of alkali equal to 0.5 wt% and up to values equal to 2.0 wt%. Furthermore, there is a difference in the effect of changing the value of σ – namely, in the case of caustic soda solution NaOH, starting from the value of concentration equal to 2.0 wt% there is almost a tenfold increase in σ up to values 0.01 mN/m, whereas in the case of Na_2CO_3 solution and at high values of concentration the surface tension values remain stably low.

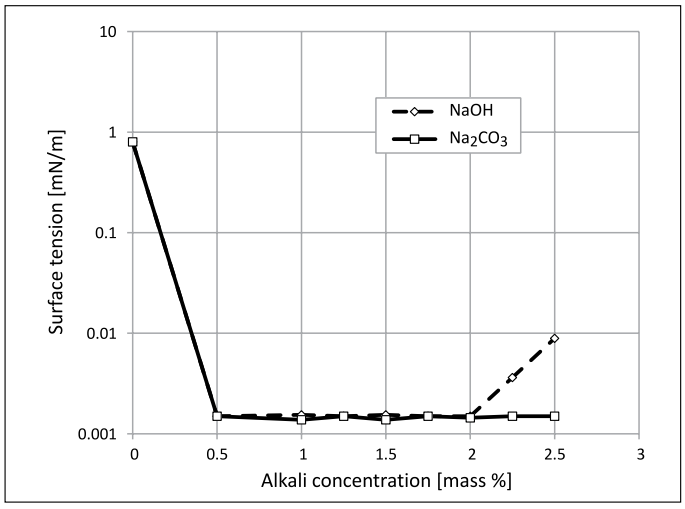

Figure 1. Dependence of the surface tension at the "oil-alkali solution" interface on the concentration of NaOH and Na_2CO_3

Rysunek 1. Zależność napięcia powierzchniowego na granicy „olej-roztwór zasadowy" od stężenia NaOH i Na_2CO_3

The results indicate that when using higher concentrations (2–4 wt%) of alkaline solutions is justified in terms of changing the wettability of the hydrophobized surfaces of the porous medium, the use of soda ash solution as an alkaline agent may be more effective and preferable.

Thus, as shown by the results of the laboratory tests above, the generation of CO_2 in the reaction of the alkaline solution with the naphthenic components (as a gas with a relatively high solubility factor in oil) can make an extra contribution to the regulation of surface tension in porous media.

When solving applied problems, it is important to identify the joint effects that reduce the surface tension at variable thermobaric and concentration parameters. With increasing pressure, the surface tension at the fluid interface decreases and depends on the value of the steady state pressure (Pasquier et al., 2017; Dimov, 2019).

$$\sigma_p = \sigma - \frac{10^{-3} abp}{1 + 10^{-5} bp + 10^{-10} cp^2}$$

where:

σ – surface tension at atmospheric pressure,

a, b, c – constants,

p – pressure.

With an increase in temperature, the surface tension also decreases $\sigma = 0$ at a critical temperature. The dependence of surface tension on temperature is given by the formula (Pasquier et al., 2017).

$$\sigma_T = 10^{-3}\,\sigma_0\,(1 - T/T_{cr})^n$$

where σ_0, n are constants for a given fluid, for example, for n-paraffins $\sigma_0 = 54.29$; $n = 1.26$.

Dependence of the oil surface tension on the pressure at the boundary with the gas phase is even more complicated. Although its general nature remains the same as for water, quantitative changes at the gas boundary for oil with increasing pressure depend on a number of factors – the chemical composition of oil, dissolved gas and its content, the nature of polar components and its volume. The higher the solubility of the gas, the more intensively the surface tension of the oil decreases with increasing pressure (Peters, 1931; Saha et al., 2018) (Table 1).

Table 1. Water surface tension at the boundary with gas phase at different temperatures and pressures

Tabela 1. Napięcie powierzchniowe wody na granicy z fazą gazową w różnych wartościach temperatury i ciśnienia

Pressure [MPa]	Surface tension in mN/m at temperature [°C]		Pressure [MPa]	Surface tension in mN/m at temperature [°C]	
	25	65		25	65
0	–	67.5	6.92	55.9	50.4
0.69	71.1	63.2	10.30	51.6	46.5
1.72	65.5	58.8	13.76	47.9	42.3
3.45	61.6	55.5	18.64	44.1	39.5

Considering the effect of surface tension reduction at the fluid interface in a porous medium, it should be noted that the process of involvement of immobilized oil in the total flow of displaced fluids depends on a number of factors. Involvement of the immobilized oil in the flow depends both on the speed of the displacing water flow and on the possibility of reducing the characteristic capillary pressure, which takes place when meniscuses of immiscible fluids move along the walls of the pore channels.

To confirm the assumptions made, we have conducted laboratory studies on an experimental model (simulating pore channels) in the form of a vertical capillary with diameter $d = 1$ mm and supporting medium with diameter $d = 4$ mm, which with proper adjustment created a working cell (Figure 2).

The main sets of experiments were carried out for the free surface of water and aqueous solutions of alkalis and surfactants. The choice of water was brought about by the fact that, due to its high surface energy, it creates conditions for maximum adsorption of the dissolved impurities in the volume.

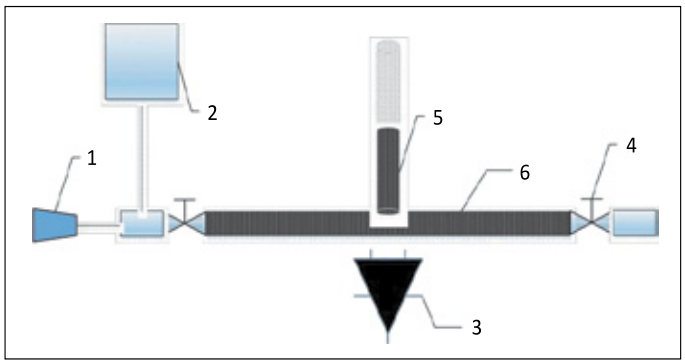

Figure 2. Experimental setup: 1 – pressure sensor; 2 – pressure source; 3 – video camera; 4 – valve; 5 – capillary tube; 6 – tube

Rysunek 2. Układ doświadczalny: 1 – czujnik ciśnienia, 2 – źródło ciśnienia, 3 – kamera wideo, 4 – zawór, 5 – rurka kapilarna, 6 – rurka

In the first series of lab experiments, an oil sample from the Binagady-North oil field (Azerbaijan) was used as displacing fluid and water was displaced from the capillary under different inlet pressures (Figure 3). During the next series of tests, an aqueous solution of surfactant (*Sulfonol* type) of small concentration (0.07%) was used. The temperature control was performed at a temperature of $T = 30$°C. In the third series of experiments, a 2% aqueous alkali solution (Na_2CO_3) was used as a displacing fluid to displace oil sample. In these experiments, it was found that the surface tension in the capillary varies depending on the pressure (Figure 3).

The task of controlling the hydrodynamic situation at the displacement front is related to creating conditions for enhancing the effect of engaging the trapped oil. This is possible both by reducing surface tension and by overcoming capillary pressure at a distance from the pressure source.

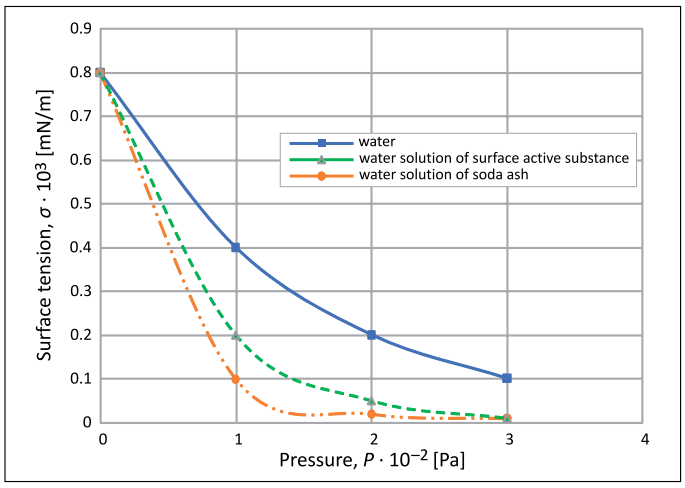

Figure 3. Dependence of surface tension on pressure

Rysunek 3. Zależność napięcia powierzchniowego od ciśnienia

Capillary effects in porous media

Oil displacement, especially of high-viscosity oil, is an unstable process and leads to the splitting of the reservoir into separate oil-saturated zones. It is traditionally assumed that fluid displacement in heterogeneous porous medium is governed by capillary forces at the interface, which, in turn, depend on the surface tension on the interface σ, the wetting angle on the contact line of both phases with the capillary surface θ and the pore space structure. In a heterogeneous medium with complex filter-capillary structure these parameters and corresponding to them capillary pressure P_k' differ for both phases. Depending on their size and pressure gradients, numerous isolated zones with residual oil saturation are formed, in which fluids may remain in a immobile, capillary-locked state, being in dynamic equilibrium with the surrounding filtration water flow.

It was shown in a study by Peters (1931) and Dimov (2019) that under capillary pressure displacing phase only arbitrarily occupies capillaries and hydrophilic pores with radii larger than critical one. At low rates oil saturated pore channels remain immobile under capillary forces.

The latter can be represented as follows: the pore channels containing the immobile oil phase have sizes that are within $r_{k_1} \le r \le r_{k_2} = \sigma\cos\theta/\Delta P = \left|\sigma\cos\theta k f_2/\mu v_0\right|$ (Dimov, 2019). Here r_{k_1} and r_{k_2} – minimum and maximum radius of pores with immobile oil; $(\sigma\cos\theta k f_2/\mu)$ is a constant value. It can be seen that with a decrease in the filtration rate, the size of the pore channels with immobile oil increases.

At the same time, “breakthrough fingers” arise on the displacement front. Structures of increasing complexity are formed, as is the case with viscous fractals or dominant instability (Li et al., 2013; Dimov, 2019; Ren and Duncan, 2019; Zhu et al., 2019). The degree of hydrodynamic instability of these structures is estimated by the Lyapunov method and the Hausdorff–Besikovich dimension (Zeitler, 1993; Blanchini et al., 2013).

On the other hand, as the applied pressure and filtration rate increase, an increased number of pore channels begin to engage in displacement (Pasquier et al., 2017; Hasanov et al., 2018). It was found that with increasing filtration rate, the instability wavelength decreases (Sabitov and Sharafutdinov, 1999; Weijermars and van Harmelen, 2017; Dimov, 2019).

It should be noted that, in the case of displacement under the hydrodynamic pressure drop, the nature of the phase distribution depends on the capillary number N_c, which is estimated by the ratio of viscous forces to capillary ones: $N_c = \mu_\beta v_\beta/\sigma$ (Brusilovsky and Zazovsky, 1991; Clark and Kleinberg, 2002; Amaral Anderson et al., 2008).

The capillary number can also be considered as $N_2 = k_0\Delta P/\sigma l$, where k_0 is the permeability; ΔP – pressure drop; l is the filtration length. These forms of capillary number are not equivalent. It follows from Darcy's law:

$$v_B = \frac{k_0}{\mu_\beta} f_\beta \frac{\Delta P}{l},\ v_\beta\mu_\beta = k_0\mu_\beta\frac{\Delta P}{l}$$

or

$$N_1 = \frac{v_\beta\mu_\beta}{\sigma} = \frac{k f_\beta \Delta P}{\sigma l} = f_\beta N_2$$

where f_β is the relative phase permeability for water; f_β – is considered as a function of mobile oil saturation. Taking into account the pore space, this dimensionless complex serves as an analogue of the capillary number N_c and is defined as (Brusilovsky and Zazovsky, 1991; Clark and Kleinberg, 2002; Amaral Anderson et al., 2008):

$$N_1' = \frac{v_\beta\mu_\beta l_k}{\sigma\cos\theta\sqrt{mk_0}}$$

To overcome capillary pressure some distance from the well, it is necessary to generate additional “local” pressure. It is known that at a constant flow rate in the injection well the filtration rate will decrease with the distance R from the well according to the law $v = Q/2\pi Rm'$, where m' is the open porosity of the formation. In this case, as a consequence, the “local” pressure at the displacement front will also decrease.

When waterflooding an inhomogeneous reservoir, the residual oil saturation of the reservoir zones with worse reservoir properties is significantly higher than the oil saturation of the basic flooded area, so the efficiency of a cyclic waterflood is higher than the efficiency of a conventional waterflood in inhomogeneous reservoirs. When the pressure increases, the elastic forces of the reservoir and fluid help the water penetrate the zones of formation with lower reservoir properties, while capillary forces retain water penetrated into the formation during a subsequent reduction in reservoir pressure. Under the influence of sign-variable pressure gradients, redistribution of fluids in the unevenly saturated reservoir occurs, aimed at equalising saturation and eliminating capillary disequilibrium at the contact point between oil-saturated and waterflooded zones, layers, areas. The pressure variations between reservoirs of different saturations accelerate capillary, countercurrent water saturation of oil-saturated zones. There is water inflow from water-saturated zones into oil-saturated zones through shallow pores, and oil flows from oil-saturated zones into water-saturated ones through large pore channels.

Under small hydrodynamic pressure gradients, the rate of meniscus movement in some of the pores is less than the rate of meniscus flow under the influence of capillary differential. In some of the larger pores, the hydrodynamic pressure drop is sufficient to push the entrapped phase and involve it in the total filtration flow. As the pressure gradient increases, an increasing proportion of pores are covered by purely hydrodynamic displacement and the volume of trapped saturation decreases.

In highly heterogeneous reservoirs, sufficient volume and area coverage occurs during development to increase overall oil recovery.

To solve the problem of increasing the sweep efficiency of zones with poor reservoir properties (immobile zones), the method of cyclic (pulse) impact on the reservoir is widely used (Nowak, 1953; Zhu et al., 2019; Czupski et al., 2020). It should be noted that implementing the technique in the field does not always lead to positive results. The disadvantage of this type of reservoir stimulation is that water can not be retained in the microfluidic zones by capillary forces in the pressure-reducing phase of the cycle. As a result, the trapped oil remains in the pores and does not infiltrate into the fluid flow (Pruess and Narasimhan, 1985). This has spurred research to develop new, more effective methods of reservoir stimulation.

This paper proposes a technological solution to increase efficiency of oil displacement sweep efficiency by creating periodically increasing hydrodynamic pressure to overcome resistance of capillary forces along the extent of the injection zone. Schematically, changing water injection pressure can be represented as the following algorithm of pressure variation (Figure 4).

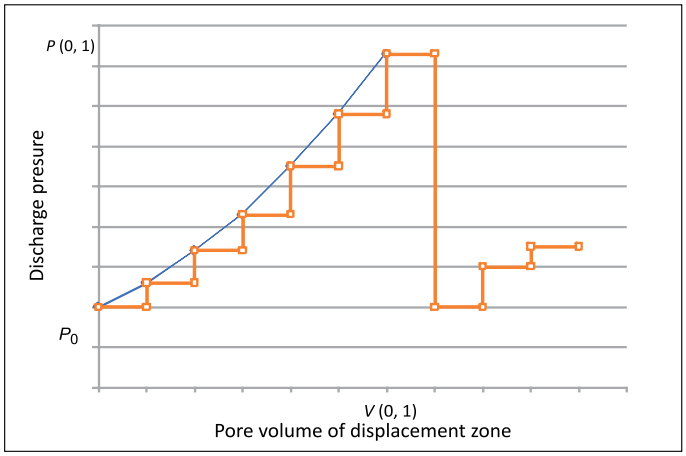

Figure 4. Injection pressure algorithm for water injection pressure control

Rysunek 4. Algorytm kontroli ciśnienia zatłaczania wody

As the injection rate changes, the velocity of pressure distribution in heterogeneous zones will vary due to differences in their reservoir properties, and consequently oil may flow from less permeable zones to more permeable watered layers. And conversely, water may flow from more permeable zones to less permeable ones, reducing the phase permeability of the formation for water and increasing it for oil.

During the pressure increase phase, the oil in the immobile pores of the reservoir gives up the space it occupies to water. Accordingly, at a distance away from the well, the content of the porous volume expands due to pressure reduction in those inhomogeneities in which water is held by capillary forces in the pores into which it has penetrated. Therefore, conditions are in place for the release of the oil phase into the mobile zone of the reservoir.

Core flow test

To confirm the assumptions put forward, oil displacement from a heterogeneous porous medium was experimentally simulated. Flow lab tests were carried out on the oil reservoir simulator CoreTest Systems FFES 655 (Figure 5).

The high-pressure column (Figure 2) was filled with a mixture of quartz sand (90%) and clay of the montmorillonite group (10%). After equipment bundling according to the above scheme, with constant temperature control (T = 323 K), the installation was vacuumized and the porous medium was saturated with water – the pore volume was equal to 0.3 m^3. Binagadi field (Azerbaijan) oil was used as an oil sample (ρ = 932–940 kg/m^3, η = 99.8–99.9 MPa·s; content of organic acids – 0.5–1.0 mg KOH/g).

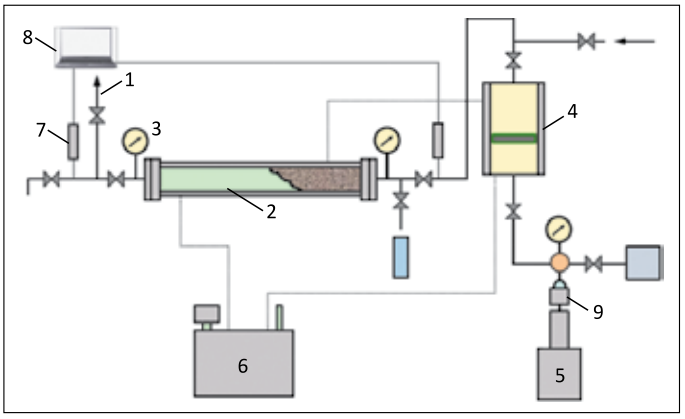

Figure 5. Scheme of the experimental setup: 1 – vacuum line; 2 – porous medium; 3 – standard pressure gauge; 4 – PVT-cell; 5 – measuring press; 6 – ultrathermostat; 7 – pressure sensor; 8 – monitor; 9 – manifold

Rysunek 5. Schemat układu doświadczalnego: 1 – przewód podciśnienia, 2 – ośrodek porowaty, 3 – manometr standardowy, 4 – ogniwo PVT, 5 – prasa pomiarowa, 6 – ultra-termostat, 7 – czujnik ciśnienia, 8 – monitor, 9 – kolektor

The value of residual water saturation was estimated in the range of 20% and the oil saturation of the model was taken as 80%. The displacement experiments were carried out in three stages. In the first stage, oil displacement with water from the Binagadi field at a constant pressure drop of 1.5 MPa (at inlet pressure – 8.0 MPa, at outlet – 6.5 MPa) was performed as a background study. When the maximum displacement coefficient was reached and the filtration process was stabilised, the water relative permeability was determined (Table 2).

Table 2. Process parameters for the oil displacement experiment
Tabela 2. Parametry procesu w eksperymencie wypierania ropy

Temperature [°C]	67	Oil phase permeability at K_o [mD]	54.3
Reservoir pressure [MPa]	7	Phase permeability to water at K_{oi} [mD]	2.2
Rock pressure [MPa]	30	Phase permeability to water at K_{of} after exposure [mD]	1.6
Oil model viscosity [cP]	1.68	Displacement mode [cm^3/min]	0.10
Reservoir mineralization. water [g/l]	22	Observed GradP on the model during displacement [MPa/m]	0.47
Displacing agent – water [g/l]	22.0	Observed GradP on the model during displacement after impact [MPa/m]	0.62

During the second stage, under similar conditions, oil was displaced by a 2% aqueous solution of soda ash (Na_2CO_3), and in the third stage displacement by aqueous solution of soda ash was carried out by changing the hydrodynamic mode – i.e., when constant values of displacement coefficient were reached, the hydrodynamic mode was changed by successive step-by-step increasing of injection pressure by aqueous solution of soda ash at the model inlet. The water displacement mode was defined based on the condition of residual oil displacement at higher values of water injection pressure. For this purpose, the pressure at the inlet of the filtration model was increased stepwise up to P_i = 7.06; 7.12; 7.18 MPa and the change in pressure difference between the inlet and the outlet of the filtration model was monitored.

The results of the lab experiments are shown on Figure 6. The above dependence describes the change in differential pressure at different displacement rates – during the water-free stage the differential pressure increases up to a certain value and decreases to 0.02 MPa when the water content increases. After changing the hydrodynamic mode, the transition to the initial displacement mode is accompanied by relatively higher values of pressure drop in the stabilisation area and significant fluctuations of ΔP, which may indirectly indicate a change in the local hydrodynamic situation in the porous medium and the connection of pore channels and capillaries not covered by displacement.

In all cases, displacement was performed by continuous injection of solutions in at least 3 times the pore volume. The research results shown on Figure 7 are the dependence of oil saturation on the volume of fluid recovered. As can be seen, there is a difference in the change in oil saturation upon oil displacement with a 2% aqueous solution of soda ash (Na_2CO_3) and with a sequential gradual increasing of injection pressure at the inlet of the model. The change is due to the fact that the displacement of oil with aqueous soda ash solution in the mode of increasing hydrodynamic pressure shows a much greater decrease in oil saturation, which indicates a better washing-out of the oil-saturated layer. In this case, there is also a relatively high water-free recovery factor. Stably low values of interfacial tension during displacement can also be explained by a chemical reaction between the alkali solution and the naphthenic components of highly resinous oil. An additional contribution to this process is made by the release of carbon dioxide (CO_2) during the reaction (Panahov et al., 2021a). Chemical reaction between oil and an aqueous solution of soda ash leads to intense gas release in the entire volume of the mixture, which is followed by gas saturation of formation fluid and generation of gas-liquid mixture under a wide contact surface of oil and alkali solution in the porous medium.

An additional factor is the control of the hydrodynamic behaviour at the displacement front to enhance the effect of

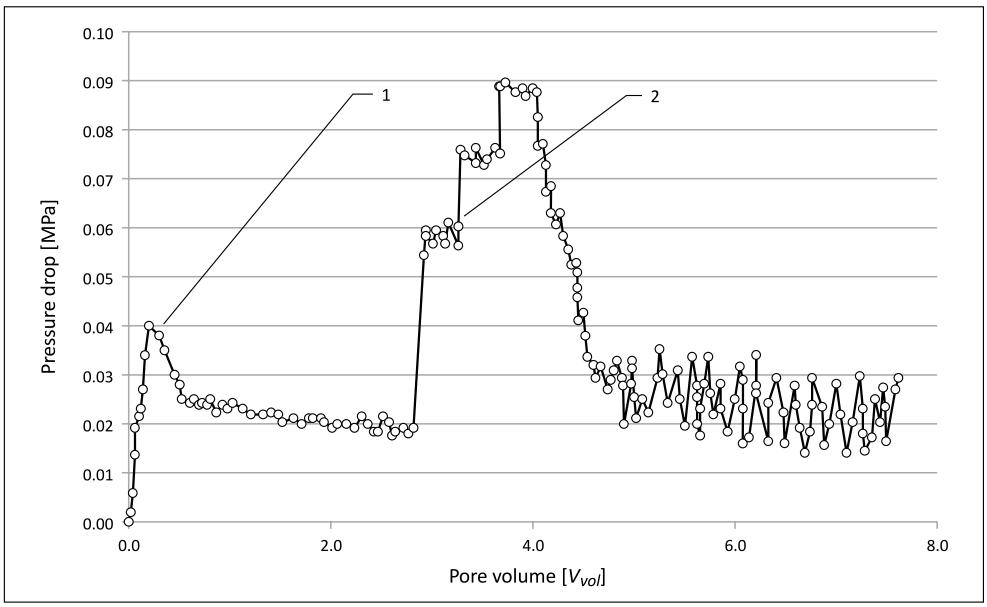

Figure 6. Dynamics of oil displacement an aqueous solution of soda ash at various hydrodynamic pressure modes (permeability k_g = 423.7 mD); 1 – displacement mode at a constant discharge pressure; 2 – displacement mode with increasing injection pressure

Rysunek 6. Dynamika wypierania ropy przez wodny roztwór sody kalcynowanej przy różnych trybach ciśnienia hydrodynamicznego (przepuszczalność k_g = 423,7 mD), 1 – tryb wypierania przy stałym ciśnieniu zatłaczania, 2 – tryb wypierania przy wzrastającym ciśnieniu zatłaczania

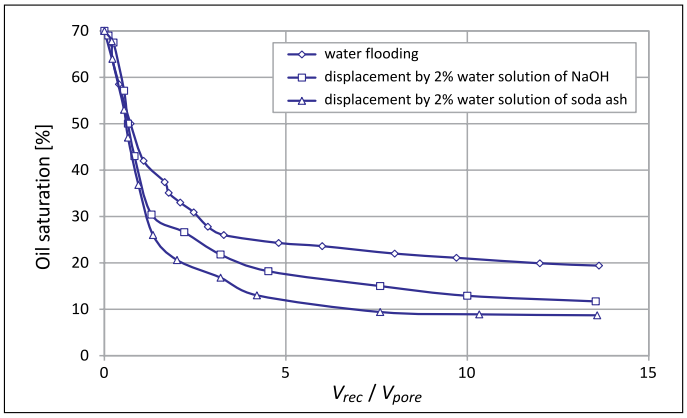

Figure 7. Change in oil saturation of a porous medium during oil displacement

Rysunek 7. Zmiana nasycenia ośrodka porowatego ropą podczas jej wypierania

engaging the oil trapped in the pores in the flow both by reducing surface tension and by overcoming the capillary pressure at a distance from the pressure source (Figure 7, curve 3).

Theoretical analysis

To estimate the effect of water intrusion acceleration in zones not covered by displacement (heterogeneous reservoir), we will use a linear equation with constant coefficients:

$$du/dt = au + f, \quad u(0) = e \tag{1}$$

Let us perform the Laplace transformation

$$\int_0^\infty e^{-st}\frac{du}{dt} = a\int_0^\infty e^{-st}udt + \int_0^\infty e^{-st}fdt \tag{2}$$

Hence, integrating by parts, we obtain

$$e^{-st}u\Big|_0^\infty + s\int_0^\infty e^{-st}udt = a\int_0^\infty e^{-st}udt + \int_0^\infty e^{-st}fdt \tag{3}$$

by introducing the notation

$$L(u) = \int_0^\infty e^{-st}udt,\ L(f) = \int_0^\infty e^{-st}fdt$$

we find

$$L(u) = \frac{c}{s-a} + \frac{L(f)}{s-a}$$

Applying the inverse Laplace transformation and the convolution theorem, we have the equation

$$u(t) = f(t) + \int_0^t u(t-s)dG(s) \tag{4}$$

where the integral is the Stieltjes integral. If $G(s)$ there is a step function with discontinuities at a finite number of points $0 < t_1 < t_2 < \ldots < t_k$, then equation (4) can be written as

$$u(t) = f(t) + \sum_{i=1}^{k} g_i u(t-t_i) \tag{5}$$

and $u(t) = 0$ for $t < 0$.

The solution obtained by Laplace transformation

$$u(t) = \int_{(G)} \frac{L(f)e^{st}ds}{1 - L(dG)}$$

can be written as

$$u(t) = \int_{(G)} \frac{L(f)e^{st}ds}{1 - \sum_{i=1}^{N} g_i e^{-st_i}}$$

where g_i are jumps.

If $\exists c_1 = \text{const} > 0$ that $|f(t)| \le c_1$ on the interval $[0, t_0]$, then there is a unique solution of the equation on $0 \le t \le t_0$. To prove it, we can use the successive-approximation method

$$u_0(t) = f(t)$$

$$u_{n+1}(t) = f(t) + \int_0^t u_0(t-s)\varphi(s)ds$$

A condition is also needed here $\int_0^{t_0} |\varphi(s)|\, ds < \infty$.

There are two sub-cases – either the numbers t_j are commensurable, or they are not commensurable. If the numbers t_j are commensurate, then the action of the root $S = r$ corresponds to a set of roots located at equal distances from each other $S = r \pm iktT_0$, $k = 1,2\ldots$. Therefore, if we assume that there is one simple real root r, then $u(t)$ has the form

$$u(t) = \sum_{k=-\infty}^{\infty} \frac{\left\{\int_0^\infty f(t_1)\exp 1 - (r + ikT_0)t_i dt_i\right\}\exp\{(r + ikT_0)i\}}{\sum_{i=1}^{N} g_i t_i e^{-rt_i}}$$

To justify the contour shift, we use Wiener's theorem. If the numbers are t_i incommensurable, then we use the results of Bochner and Pitt (Rao, 1997).

Let us now consider equation (1). Take the function $P(t)$ as follows – let $P(t)$ be the simplest discontinuous function, such as a step function. Consider the derivative of a piecewise absolutely continuous function $P(t)$ with a piecewise continuous derivative $P'(t)$, discontinuity points $t_1, t_2,\ldots$ and corresponding jumps $h_1, h_2,\ldots$.

We introduce the function

$$P_1(t) = P_1(t) - \sum_k h_k \cdot \theta(t - t_k)$$

where $\theta(t) = \begin{cases} 1, & t > 0 \\ 0, & t < 0 \end{cases}$

It is known that $\theta'(t) = \delta$, i.e. $\theta(t)$ in the usual sense is 0 at $t \neq 0$, and does not exist at $t = 0$. The function $P_1(t)$ is absolutely continuous and recoverable from its derivative $P'_1(t)$, coincides with $P'(t)$ everywhere except at the discontinuity points $P(t)$, where $P'(t)$ it does not exist. Therefore, $P'_1(t)$ there is a deriva-

tive of a generalised function P_1 in the space of generalised functions. On the other side

$$P_1'(t) = P'(t) - \sum\nolimits_k h_k \cdot \delta(t - t_k)$$

where f' is the derivative of the generalised function $P(t)$. As a result, we get

$$P'(t) = P_1'(t) + \sum\nolimits_k h_k \cdot \delta(t - t_k) \tag{6}$$

i.e. the derivative of the generalised function $P(t)$ is recovered from its ordinary derivative and the sum of the delta function at discontinuity points with the corresponding jumps.

Further, the general solution of equation (1) will be in the form

$$v = \frac{1}{\exp\left(\dfrac{\alpha t}{\mu\beta_2}\right)}\left\{\frac{\alpha}{\mu}\int\left[P_1'(t) + \sum\nolimits_k h_k \cdot \delta(t - t_k)\right]dt + c\right\} \tag{7}$$

It is important to control the pressure distribution in the reservoir zones when investigating the rising injection pressure mode. Pressure redistribution after injection with constant flow rate until the next cycle looks like flat-radial filtration (Mirzajanzadeh and Shakhverdiev, 1997):

$$\frac{\partial P}{\partial t} = \chi\left(\frac{\partial^2 p}{\partial r^2} + \frac{1}{r}\frac{\partial P}{\partial r}\right) \tag{8}$$

with initial and boundary conditions:

$$P(r,t) = P_{k_i} = \text{const at } t = 0$$

$$Q_1 = \frac{2\pi kh}{\mu}\left(r_1\frac{\partial P}{\partial r}\right)_{r=r_1}$$

$$Q_1 = 0 \text{ at } r = 0;$$

$$P(r,t) = \left(P_{k_i} - \frac{Q\mu r}{\omega k}\right)_{r=r_1}$$

where is the Q_1 – flow rate, t – time, χ – piezoconductivity.

The exact solution has the following form (Pruess and Narasimhan, 1985; Mirzajanzadeh and Shakhverdiev, 1997):

$$P_{k_i} - P(r,t) = \frac{Q\mu}{4\pi kh}E_i\left(-\frac{r^2}{4\chi t}\right) \tag{9}$$

where P_{k_i} is the injection pressure.

As shown in (Pruess and Narasimhan, 1985; Meng and Ju, 2022) for small values:

$$E_i\left(-\frac{r^2}{4\chi t}\right) = \int_{\frac{r^2}{4\chi t}}^{\infty}\frac{l^4}{u}\,du = \ln\frac{4\chi t}{r^2} - 0.5772$$

From (9) we get

$$P_{k_i} - P(r,t) = \frac{Q\mu}{4\pi kh}\left(\ln\frac{4\chi t}{r^2} - 0.5772\right) \tag{10}$$

The pressure at any point in the reservoir at any time during the injection of an elastic fluid parallel to the OX axis at a constant pressure $(P_{k_i} - P_{k_{(i-1)}})$ and flows in an unsteady mode can be obtained by integrating the equation:

$$\frac{\partial P}{\partial t} = \chi\frac{\partial^2 P}{\partial x^2} \tag{11}$$

under initial and boundary conditions

$$P(x,0) = 0 \text{ at } t = 0$$

$$P(0,t) = P_k \text{ for } x = 0 \tag{12}$$

$$v(0,t) = \text{const};\ P(x,t) = \left(P_{ki} - \sqrt{\frac{3}{2}}\frac{\mu\sqrt{\chi t}}{k}v\right), \text{ for } x = \infty$$

Due to the difficulty of exact solutions and in order to make estimates of equation parameters available, various methods for solving problems of non-steady-state flow of elastic fluid have been proposed.

One of the most common approximate methods is the technique of successive change of stationary states (Meng and Ju, 2022). If at each stage of fluid injection the flow rate does not change with time, i.e.:

$$Q(0,t) = \text{const}$$

$$P(x,t) = (P_{k_i} - P_f)\frac{x}{l(t_i)} \tag{13}$$

where:

P_{k_i} – injection pressure,

P_f – pressure on the flow path.

As is known (Teklu et al., 2013), the distribution of the displacement front may be described as

$$\Delta P_f = (P_{k_i} - P_f) = \sqrt{\frac{3}{2}}\frac{\mu}{k}v\sqrt{\chi t} \tag{14}$$

Under the condition $P_f > P'_k$ of possible fluid exchange between the immobile and mobile zones of the reservoir, where $P'_k = (2\sigma\cos\theta)/r$.

The terms provided on the radius of the contour $P_f \le P'_k$ are that once again it is necessary to increase the pressure at the injection inlet.

The pressure propagation time is estimated as

$$t = \left[\frac{(P_{k_i} - \mathrm{P}_f)k}{\mu\chi\sqrt{3/2}}\right]^2 \tag{15}$$

With known reservoir parameters, it is possible to determine the radius of influence. The reduced impact radius is determined from the material balance equation and known from t (11) (Meng and Ju, 2022):

$$l(t) = \sqrt{6\chi t} = \sqrt{6\chi}\frac{(P_{k_i} - \mathrm{P}_{k(i-1)})k}{\mu\chi\sqrt{3/2}} \tag{16}$$

where $\chi = kK/\mu m$; $K = m/\beta^*$, where $\beta^* = m\beta_f + \beta$ is the compressibility coefficient of the fluid and porous medium. With known (13), (14), (15) and from (15), one can estimate $P(x, t)$.

Fluid exchange between the mobile and immobile zones occurs due to an increase in the average pressure drop between them. The task considered above is performed technologically in the following steps:

- at time $t = 0$ in the discharge gallery, the pressure instantly rises from P_0 to P_1 and for some period of time t_1 is kept constant. The operational gallery continues to operate as before;
- at time $t = t_1$ water continues to be pumped into the injection well, thereby instantly increasing the pressure at its bottomhole to a value of $P = P_2$;
- the second stage continues for some time t_2, after which the 1st, 2nd, etc. are repeated again. stages (k_i), $i = 1, 2, \ldots, n$;
- at the last stage of exposure (k_n) at the end of the time interval t_i the pressure is reduced to the initial (i.e. reservoir) level P_0;
- the above steps are repeated.

The operating conditions required to implement the technology solution in the field must also be determined: a) distribution of increased pressure at any point of the immobile and mobile zones of the reservoir at any time at all stages of pressure control; b) the injection phase time; c) average capillary pressure P'_k.

With known reservoir characteristics, conditions (a), (b) and (c) are estimated as follows: the "replacement pressure" or radius of the next pressure stage of countercurrent capillary impregnation is determined with the following geological and physical characteristics of the formation (Glotov, 2021):
$k = 400$ mD; $m = 0.15$; $\sigma = 35 \cdot 10^{-6}$ kg/sm $= 34.4 \cdot 10^{-3}$ N/m; $\cos\theta = 0.6$; $\mu = 1.2 \cdot 10^{-3}$ · Pa·s; $\beta_c = 0.306 \cdot 10^{-10}$ m^2/n; $\beta_f = 4.59 \cdot 10^{-10}$ m^2/n; P_i – 20 MPa; $t = 3$ days; $Q = 100$ m^3/day; $B = 250$ m; $h = 10$ m;

$$l(t) = \sqrt{6\chi t};\ t = 3 \text{ days} = 3 \cdot 0.864 \cdot 10^5 = 2.6 \cdot 10^5 \text{ s};$$

$$\chi = \frac{k}{\mu(m\beta_f + \beta_c)} =$$

$$= \frac{0.4 \cdot 1.02 \cdot 10^{-12}}{1.2 \cdot 10^{-3}\left(0.15 \cdot 4.59 \cdot 10^{-10} + 0.306 \cdot 10^{-10}\right)} = 3.42 \text{m}^2/\text{s};$$

$l(t) = 2.3 \cdot 10^3$ m;

$P(x,t) = 20 - (20 - P_f)(x / l(t))$;

$$(20 - P_f) = \sqrt{\frac{3}{2}\frac{1.2 \cdot 10^{-3}}{0.4 \cdot 1.02 \cdot 10^{-12}} \cdot 9.4 \cdot 10^2 \cdot v};$$

$$v = \frac{100}{250 \cdot 10} = 0.04\frac{\text{m}}{\text{day}} = 4.6 \cdot 10^{-7} \text{ m/s};$$

$$(20 - P_f) = 1.225 \cdot \frac{1.2 \cdot 10^{-3} \cdot 9.4 \cdot 10^2 \cdot 4.6 \cdot 10^{-7}}{0.4 \cdot 1.02 \cdot 10^{-12}} =$$

$$= \frac{1.2 \cdot 10^2 \cdot 9.4 \cdot 10^2 \cdot 4.6}{0.4 \cdot 1.02} \cdot 1.225 = 156 \cdot 10^4 = 1.6;$$

$P(x,t) = 20 - (20 - P_f)\, x / l(t)$;

$$P(x,t) = 20 - 1.6 \cdot \frac{x}{2.3 \cdot 10^3} = 19.99;$$

$x = 1$ $\quad P(x,t) = 19.99$
$x = 10$ $\quad P(x,t) = 19.98$
$x = 100$ $\quad P(x,t) = 19.90$
$x = 1000$ $\quad P(x,t) = 19.30$

$$\text{At } v = \frac{100}{100 \cdot 10} = 0.1\frac{\text{m}}{\text{day}} = 0.12 \cdot 10^{-5} \text{ m/s};$$

$$(20 - P_f) = 1.225 \cdot \frac{1.2 \cdot 10^{-3} \cdot 9.4 \cdot 10^2 \cdot 0.12 \cdot 10^{-5}}{0.4 \cdot 1.02 \cdot 10^{-12}} =$$

$$= 4.06 \cdot 10^6 = 4.06 \text{ MPa};$$

$$P(x,t) = 20 - 4.06\frac{x}{l(t)};$$

$x_1 = 1$ $\quad P(x,t) = 19.99$
$x_1 = 10$ $\quad P(x,t) = 19.98$
$x_1 = 100$ $\quad P(x,t) = 19.80$
$x_1 = 1000$ $\quad P(x,t) = 18.20.$

Thus, the calculated example makes it possible to estimate pressure distribution along the reservoir in discrete sections of the reservoir as the displacement front advances and, thus, the time frame of hydrodynamic pressure drop change. This makes it possible to determine the duration and stage of injection pressure control in order to reach the expected hydrodynamic effect and, consequently, to increase oil flow to the gallery of producing wells.

Field cases

Laboratory studies served as the basis for the field implementation of the technological solution impact on a heterogeneous reservoir with residual, stagnant oil-saturated areas. The method has found application in the course of a technological operation on a group of wells operated offshore by the Bohai Bay oil field Company CNOOC (PRC) (Panahov et al., 2021b). The treatment was carried out on the site of the deposit, covering 14 production wells that respond to water impact. The technology was implemented with the support of the New Horizon company at the C12 injection well (Figure 8):

At the end of the field operation, the injection pressure and injection volume with an aqueous solution of Na_2CO_3 were monitored at the injection well (Figure 9).

According to the indicators of the responding wells in the area of technology implementation, a positive response to hydrodynamic impact is shown for all wells in general, with an increase or stabilisation of the average daily oil flow rate for the majority of production wells. The well performance of oil production rates and water cut of the C54ST2 well (Penglai oil field, China) after the treatment operation are shown in Figure 10.

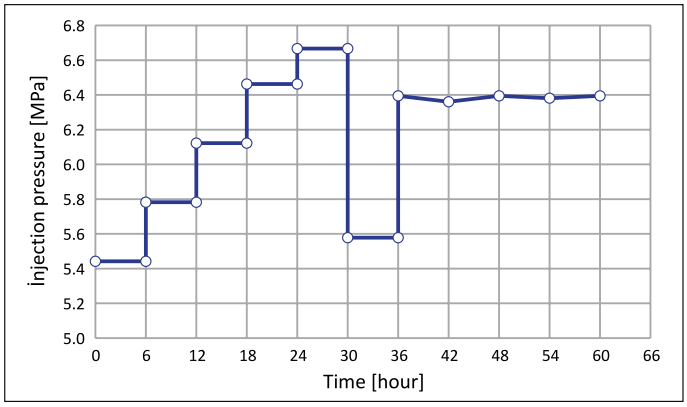

Figure 8. Pressure changes algorithm during the treatment operation on injection well C12 (Penglai oil field, CNOOC)

Rysunek 8. Algorytm zmian ciśnienia podczas obróbki w odwiercie C12 (złoże ropy Penglai, CNOOC)

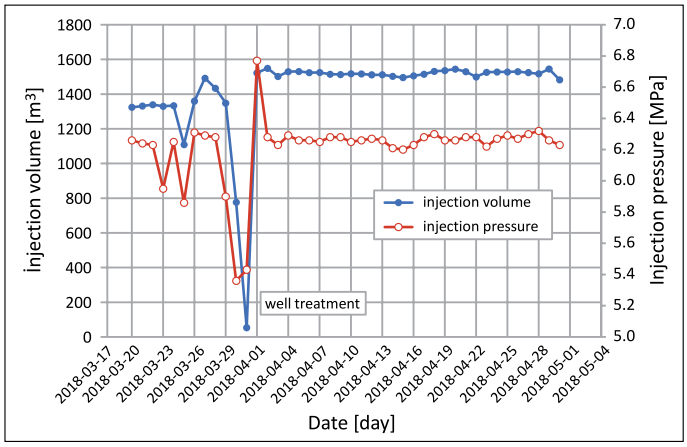

Figure 9. Changes in well performance of injection well C12

Rysunek 9. Zmiany wydajności odwiertu C12

Conclusions

1. Laboratory studies have confirmed that, along with the factors of reducing interfacial tension, emulsifying oil, changing the wettability of the rock, the interaction of the injected alkaline agent with the active acidic components of highly tarry and asphaltene oils plays a significant role in the processes of alkaline flooding.
2. Studies have shown that capillary processes and the instability of the front of oil displacement by water are important elements of the dependence of residual oil saturation on surface tension and hydrodynamic pressure in the reservoir.
3. Researches have revealed that the intensity and direction of capillary forces depend on a number of physical and physical-chemical properties of reservoir systems – reservoir, saturating fluids, including displacement conditions.
4. One way to optimise stimulation, taking into account capillary processes in the porous medium, is to minimise surface tension by using effective chemical compositions and to apply a steady, periodically increasing hydrodynamic pressure.

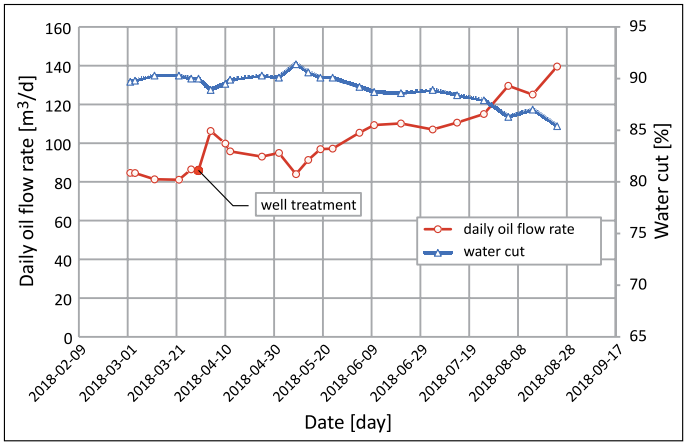

Figure 10. Average daily oil production rate and water cut in the responding well after treatment operation

Rysunek 10. Średni dzienny poziom wydobycia ropy i wody w odwiercie po zabiegu oczyszczania

References

Amaral Anderson da S., Augustine J., Henriksen K., Rodrigues V.F., Steagal D.E., Paixão L.C.A. da Barbosa P., 2008. Equalization of the Water Injection Profile of a Subsea Horizontal Well: A Case History. *SPE International Symposium and Exhibition on Formation Damage Control, Lafayette, Louisiana, USA*. DOI: 10.2118/112283-MS.

Arekhov V., Hincapie R.E., Clemens T., Tahir M., 2020. Variations in wettability and interfacial tension during alkali-polymer application for high and low tan oils. *Polymers*, 12(10): 1–28. DOI: 10.3390/polym12102241.

Blanchini F., Colaneri P., Valcher M.E., 2013. A stabilizable switched linear system does not necessarily admit a smooth homogeneous Lyapunov function. *Proceedings of the IEEE Conference on Decision and Control*: 5969–5974. 10.1109/CDC.2013.6760831.

Brouwer D.R., Jansen J.D., 2002. Dynamic Optimization of Water Flooding with Smart Wells Using Optimal Control Theory. *European Petroleum Conference, Aberdeen, United Kingdom*. DOI: 10.2118/78278-MS.

Brusilovsky A.I., Zazovsky A.F., 1991. A New Approach to Modelling of Multicomponent Two-Phase EOR Processes with Interphase Mass Exchange. *SPE Annual Technical Conference and Exhibition, Dallas, Texas, USA*. DOI: 10.2118/22638-MS.

Cheshkova T.V., Arysheva A.D., Min R.S., Sagachenko T.A., 2019. Composition of asphaltenes of heavy oil residues from the Usinskoye oil field. *AIP Conference Proceedings*, 2167(1): 020054. DOI: 10.1063/1.5131921.

Clark B., Kleinberg R., 2002. Physics in oil exploration. *Physics Today*, 55(4): 48–53. DOI: 10.1063/1.1480782.

Czupski M., Kasza P., Leśniak Ł., 2020. Development of Selective Acidizing Technology for an Oil Field in the Zechstein Main Dolomite. *Energies*, 13(22): 5940. DOI: 10.3390/en13225940.

Dimov S.V., 2019. Experimental investigation of decreasing porosity and permeability of bead packing at suspension flow. *Journal of Physics: Conference Series*, 1404(1). DOI: 10.1088/1742-6596/1404/1/012015.

Glotov A.V., 2021. Residual Water Content and Water Saturation of Bazhenov Formation Cores. *SPE Symposium: Petrophysics XXI. Core, Well Logging, and Well Testing, Virtual*. DOI: 10.2118/208418-MS.

Hasanov R., Efendiyev R., Kazymov B., Guliyev A., Zeynalov A., Smirnova A., 2018. Inelastic Deformations of Rocks and their Influence on Development of the Oil and Gas Fields. *Petroleum & Petrochemical Engineering Journal*, 2(2): 1–8. DOI: 10.23880/ppej-16000161.

Islam M.R., 1991. Cosurfactant-Enhanced Alkaline/Polymer Floods for Improving Recovery in a Fractured Sandstone Reservoir. In: Sharma M.K., Sharma G.D. (eds.): Particle Technology and Surface Phenomena in Minerals and Petroleum. *Springer, Boston*: 223–233. DOI: 10.1007/978-1-4899-0617-5_16.

Jones D.M., Watson J.S., Meredith W., Chen M., Bennett B., 2001. Determination of naphthenic acids in crude oils using nonaqueous ion exchange solid-phase. *Analytical Chemistry*, 73(3): 703–707. DOI: 10.1021/ac000621a.

Larson R.G., Scriven L.E., Davis H.T., 1981. Percolatıon Theory of Two-Phase Flow in Porous Media. *Chemical Engineering Science*, 36(1): 57–73.

Lenormand R., Touboul E., Zarcone C., 1988. Numerical models and experiments on immiscible displacements in porous media. *Journal of Fluid Mechanics*, 189: 165–187. DOI: 10.1017/S0022112088000953.

Li Z., Chen H., Yu C., Du L., Qiao Y., Liu W., 2013. Hydrodynamic geological effect during the waterflooding of seriously heterogeneous reservoirs. *Petroleum Exploration and Development*, 40(2): 224–229. DOI: 10.1016/S1876-3804(13)60026-9.

Liu Q., Dong M., Ma S., Tu Y., 2007. Surfactant enhanced alkaline flooding for Western Canadian heavy oil recovery. *Colloids and Surfaces A: Physicochemical and Engineering Aspects*, 293(1–3): 63–71. DOI: 10.1016/j.colsurfa.2006.07.013.

Lyu W., Zeng L., Chen M., Qiao D., Fan J., Xia D., 2018. An approach for determining the water injection pressure of low-permeability reservoirs. *Energy Exploration and Exploitation*, 36(5): 1210–1228. DOI: 10.1177/0144598718754374.

Meng L., Ju B., 2022. Experimental Study of Water Displacement Rates on Remaining Oil Distribution and Oil Recovery in 2D Pore Network Model. *Energies*, 15(4). DOI: 10.3390/en15041501.

Mirzajanzadeh A.K., Shakhverdiev A.K., 1997. Dinamicheskie processy v neftegazodobyche. *Nauka*.

Musayev R.A., Jafarli S.Z., Xalilov E.G., Gashimov A.F., 1999. On the possibility of improving the efficiency of alkaline waterflooding of formations containing inactive oil. *Nafta Press*.

Nakoryakov V., Kuznetsov V., 1997. Capillary phenomena, heat and mass transfer and wave processes in two-phase flow in porous systems and fillings. *Applied Mechanics and Engineering Physics*, 38(4): 155–166.

Nowak T.J., 1953. The Estimation of Water Injection Profiles from Temperature Surveys. http://onepetro.org/JPT/article-pdf/5/08/203/2238788/spe-953203-g.pdf.

Panahov G.M., Abbasov E.M., Jiang R., 2021a. The novel technology for reservoir stimulation: in situ generation of carbon dioxide for the residual oil recovery. *Journal of Petroleum Exploration and Production*, 11(4): 2009–2026. DOI: 10.1007/s13202-021-01121-5.

Panahov G.M., Abbasov E.M., Jiang, R., 2021b. The novel technology for reservoir stimulation: in situ generation of carbon dioxide for the residual oil recovery. *Journal of Petroleum Exploration and Production*, 11(4): 2009–2026. DOI: 10.1007/s13202-021-01121-5.

Pasquier S., Quintard M., Davit Y., 2017. Modeling two-phase flow of immiscible fluids in porous media: Buckley-Leverett theory with explicit coupling terms. *Physical Review Fluids*, 2(10). DOI: 10.1103/PhysRevFluids.2.104101.

Peters R.A., 1931. Interfacial tension and hydrogen-ion concentration. *Proceedings of the Royal Society of London. Series A, Containing Papers of a Mathematical and Physical Character*, 133(821): 140–154. DOI: 10.1098/rspa.1931.0135.

Phukan R., Gogoi S.B., Tiwari P., 2019. Enhanced oil recovery by alkaline-surfactant-alternated-gas/CO_2 flooding. *Journal of Petroleum Exploration and Production Technology*, 9: 247–260. DOI: 10.1007/s13202-018-0465-0.

Pruess K., Narasimhan T.N., 1985. A Practical Method for Modeling Fluid and Heat Flow in Fractured Porous Media. *Society of Petroleum Engineers Journal*, 25(01): 14–26. DOI: 10.2118/10509-PA.

Rao M.M., 1997. Second order nonlınear stochastıc dıfferentıal equatıons. *Nonlinear Analysis, Theory, Methods & Applicatimu*, 30(5): 3147–3151.

Ren B., Duncan I., 2019. Modeling Oil Saturation Evolution in Residual Oil Zones: Implications for CO_2 EOR and Sequestration. *Journal of Petroleum Science and Engineering*, 177: 528–539. DOI: 10.1016/j.petrol.2019.02.072.

Rudin J., Wasan D.T., 1992. Mechanisms for lowering of interfacial tension in alkali/acidic oil systems: Effect of added surfactant. *Industrial & Engineering Chemistry Research*, 31(8): 1899–1906. DOI:10.1021/IE00008A010.

Sabitov A.R., Sharafutdinov, R. F., 1999. Thermal field of an oil bed in a nonstationary pressure field. *Journal of Engineering Physics and Thermophysics*, 72(2): 250–253. DOI: 10.1007/BF02699147.

Saffman P.G., Taylor G.I., 1958. The penetration of a fluid into a porous medium of Hele-Shaw cell containing a more viscous liquid. *Proceedings of the Royal Society of London. Series A, Mathematical and Physical Sciences*, 245(1242): 312–329. DOI: 10.1098/rspa.1958.0085.

Saha R., Uppaluri R.V.S., Tiwari P., 2018. Influence of emulsification, interfacial tension, wettability alteration and saponification on residual oil recovery by alkali flooding. *Journal of Industrial and Engineering Chemistry*, 59: 286–296. DOI: 10.1016/j.jiec.2017.10.034.

Surguchev L., Koundin A., Melberg O., Rolfsvag T., Menard W.P., 2002. Cyclic water injection: Improved oil recovery at zero cost. *Petroleum Geoscience*, 8(1): 89–95. DOI: 10.1144/petgeo.8.1.89.

Taylor K.C., Hawkins B.F., Islam R.M., Taylor K.C., Hawkins B.F., 1990. Dynamic Interfacial Tension in Surfactant Enhanced Alkaline Flooding. *Journal of Canadian Petroleum Technology*, 29(01): 50–55. DOI: 10.2118/90-01-05.

Teklu T., Brown J.S., Kazemi H., Graves R., Al Sumaiti A.M., 2013. Residual Oil Saturation Determination – Case Studies in Sandstone and Carbonate Reservoirs. *75th EAGE Conference and Exhibition Incorporating SPE Europec*. SPE-164825. DOI: 10.3997/2214-4609.20130893.

Vavra E., Puerto M., Biswal S.L., Hirasaki G.J., 2020. A systematic approach to alkaline-surfactant-foam flooding of heavy oil: microfluidic assessment with a novel phase-behavior viscosity map. *Scientific Reports*, 10, 12930. DOI: 10.1038/s41598-020-69511-z.

Weijermars R., van Harmelen A., 2017. Advancement of sweep zones in waterflooding: conceptual insight based on flow visualizations of oil-withdrawal contours and waterflood time-of-flight contours using complex potentials. *Journal of Petroleum Exploration and Production Technology*, 7(3): 785–812. DOI: 10.1007/s13202-016-0294-y.

Wojnicki M., 2017. Experimental investigations of oil displacement using the WAG method with carbon dioxide. *Nafta-Gaz*, 73(11): 864–870. DOI: 10.18668/NG.2017.11.06.
Wu C., de Visscher A., Gates I.D., 2019. On naphthenic acids removal from crude oil and oil sands process-affected water. *Fuel*, 253: 1229–1246. DOI: 10.1016/J.FUEL.2019.05.091.
Yin Z., Yuan P., Lian X., Zheng Y., Zheng H., Yin Z., Yuan P., Lian X., Zheng Y., Zheng H., 2019. Components of Paraffin-Base and Naphthenic-Base Crude Oil and Their Effects on Interfacial Performance. *Open Journal of Yangtze Oil and Gas*, 4(4): 270–284. DOI: 10.4236/OJOGAS.2019.44022.
Zeitler H., 1993. About Hausdorff-Besicovitch-dimension, *International Journal of Mathematical Education in Science and Technology*, 24(1): 63–71. DOI: 10.1080/0020739930240108.
Zhu X., Cai H., Wang X., Zhu Q., Meng Z., Zhu X., Cai H., Wang X., Zhu Q., Meng Z., 2019. Research and Application of Water Flooding Timing and Method for Blocky Bottom Water Fractured Buried Hill Reservoir. *Journal of Power and Energy Engineering*, 7(9): 1–10. DOI: 10.4236/jpee.2019.79001.

Geylani Minhac PANAHOV, Ph.D.
Head of the Department of Fluid Mechanics
Correspondent member of Azerbaijan NAS
Institute of Mathematics and Mechanics
Azerbaijan National Academy of Sciences
B. Vagabzade, 9, AZ1141, Baku, Azerbaijan
E-mail: *geylani.panahov@imm.az*

Eldar Mehdi ABBASOV, Ph.D.
Leading Researcher at the Department of Fluid Mechanics; Institute of Mathematics and Mechanics
Azerbaijan National Academy of Sciences
B. Vagabzade, 9, AZ1141, Baku, Azerbaijan
E-mail: *eldar.abbasov@imm.az*

Babek Nazim SULTANOV, M.Sc.
Senior Laboratory Scientist at the Department of Modern Geodynamics and Space Geodesy
Institute of Geology and Geophysics
Azerbaijan National Academy of Sciences
H. Javid Ave. 119, AZ1143 , Baku, Azerbaijan
E-mail: *bsaultanov@mail.ru*